



## Investigation of Surface Dose Accuracy of Two Dose Calculation Algorithms Using Thermoluminescent Dosimeters

Osman Vefa GÜL<sup>1\*</sup>

<sup>1</sup>Selçuk University, Faculty of Medicine, Department of Radiation Oncology, Selçuklu, Konya, Türkiye

Keywords	Abstract
Surface Dose Thermoluminescent Dosimetry Algorithm	Accurate estimation of the surface dose in radiotherapy is very important in reducing skin reactions. This study aims to evaluate the accuracy of two different treatment planning algorithms in calculating the surface dose in a specially designed phantom using thermoluminescent dosimetry (TLD). In this study, a special phantom was designed for surface dose measurement. The phantom surface consisted of an adhesive bolus for the adhesion of TLDs. 121 TLDs were placed 1 cm apart on the bolus surface. In TPS, irradiation plans were created at different fields and source-surface distances (SSD). Dose calculations were made with Anisotropic Algorithm algorithms (AAA) and Pencil Beam Convolution (PBC) algorithms for all plans. The mean dose was measured for each point. For each of the 4x4, 6x6, 8x8, 10x10, and 12x12 cm <sup>2</sup> domains, the TLDs within the domain were approximately 1 cm inward from the edge. To measure the effect of SSD on surface dose, the isocenter point was located at depths of 0 cm, 2.5 cm and 5.0 cm, respectively. The surface dose at each depth was measured with TLDs. The doses calculated by the AAA and PBC algorithms were compared with the doses measured by TLDs. The AAA algorithm overestimates the surface dose by 4% compared to the TLD measurement for the 4x4 field. The surface dose calculation of the PBC algorithm was found to be high when compared to TLD measurements for all SSDs and fields. There was a significant difference between the PBC algorithm dose calculation and TLD measurements in all fields and SSDs (p<0.001). It was observed that the AAA algorithm performed better in calculating the surface dose than the PBC algorithm. AAA and PBC algorithm users are advised to be more careful about surface dose calculation.

### Cite

Gül, O. V. (2023). Investigation of Surface Dose Accuracy of Two Dose Calculation Algorithms Using Thermoluminescent Dosimeters. *GU J Sci, Part A, 10(3)*, 353-360. doi:10.54287/guj.1347041

### Author ID (ORCID Number)

0000-0002-6773-3132 Osman Vefa GÜL

### Article Process

**Submission Date** 20.08.2023  
**Revision Date** 01.09.2023  
**Accepted Date** 16.09.2023  
**Published Date** 28.09.2023

## 1. INTRODUCTION

Radiation is the transport of energy in the form of waves or particles (Lejosne et al., 2022; Aydemir et al., 2023). Radiation that has the energy to remove electrons from the atom's orbit is called ionizing radiation. Radiation therapy, is aimed to destroy cancer cells by using particle or wave radiation. Ionizing radiation is used in radiotherapy, which plays a primary role in treating cancer patients. The main purpose of radiotherapy is to protect critical organs in the best possible way while delivering the required dose to the target volume (Simoni et al., 2021). Modern treatment techniques are used together with the developing technology in radiation therapy (Matsumoto et al., 2021). All current treatment techniques require a treatment planning process based on computed tomography (CT) images. Thanks to the treatment planning processes, the absorbed dose in the target volume and organs at risk can be estimated by the treatment planning systems (TPS). TPSs use different dose calculation algorithms. It is vital that these algorithms accurately estimate the dose. Algorithms used in radiotherapy successfully estimate the in-field and organ-at-risk (OAR) doses but cannot successfully calculate the out-of-field and surface doses.

\*Corresponding Author, e-mail: [vefagul@selcuk.edu.tr](mailto:vefagul@selcuk.edu.tr)

The failure of dose calculation algorithms in the superficial region is due to electron instability, multi-leaf collimators (MLC) leakage, and beamformers such as secondary collimators and blocks. It does not take into account the radiation scattered from the patient (Chakarova et al., 2012). The absorption of photon rays used in radiation therapy in the surface region varies depending on many parameters. These parameters include field size, distance from the beam source, and beam angle (Panettieri et al., 2009). Photon energies used in radiotherapy are absorbed as a result of Compton scattering. The photon beams transfer some of their energy to the orbiting electrons, and the electrons gain motion energy. The activated electrons transfer their energy to the tissue and are absorbed. As a result of this absorption, secondary radiation is transferred to the tissue. Secondary radiations generated on the surface significantly affect the skin dose (Ravikumar & Ravichandran, 2000; Mowery & Singh, 2023). Contaminated electrons in the head of the therapy device can be caused by components such as primary collimator, flattening filter, monitor ion chambers, target, and treatment set-up parameters such as field size, wedge filter, block carrier tray, patient fixation tools, and source-skin distance (SSD) (Tsapaki & Bayford, 2015; Ng et al., 2022). While the patient is irradiated, the SSD is very important for the skin dose. Skin side effects are common during radiation therapy (Ramseier et al., 2020; Córdoba et al., 2021). Side effects on the skin due to radiation adversely affect the patient's quality of life (Wang & Tepper, 2021). The field size is also one of the critical parameters affecting the skin dose. Increasing the area size causes an increase in dose in the build-up region. High-energy photons release their maximum dose ( $d_{max}$ ) more profoundly than the surface, depending on their energies. This is called the skin-sparing effect of high-energy photon beams. Although TPS can accurately estimate the dose given to the target volume and OARs, studies have shown that TPS cannot accurately calculate the surface dose (Danckaert et al., 2023). The accuracy of TPSs in calculating surface dose has been reported by various researchers on inhomogeneous phantoms. There is a lack of confidence in the surface dose calculation of TPS. Surface dose measurements require special dosimetric methods. The most important of these dosimetric equipment is in vivo dosimetry. Various measurement methods such as film dosimetry, Thermoluminescent dosimeter (TLD), diode dosimetry, semiconductor detectors and ion chambers have been developed for in-vivo dosimetry.

Few studies report comparisons of measured skin doses with doses calculated by TPS. This study aims to evaluate the accuracy of two different treatment planning algorithms in calculating the surface dose in a specially designed phantom using thermoluminescence dosimetry.

## 2. MATERIAL AND METHOD

### Phantom Design

The necessary phantom setup was created to examine the surface doses for modern radiotherapy techniques. For this setup, 10 PTW brand RW3 solid-water phantoms (PTW, Physikalisch Technische Werkstätten, Freiburg, Germany) in 40x40 dimensions were placed on each other. The RW3 phantom can be used for dose measurements for high-energy photon and electron energies. RW3 material contains  $2.1 \pm 0.2\%$   $TiO_2$  mixed polystyrene ( $C_8H_8$ ), its mass density is  $1.045 \text{ g/cm}^3$ , and its electron density is  $3.386 \times 10^{23} \text{ e/g}$  (Guardiola et al., 2022). A 0.5 cm thick gel layer-type adhesive bolus was fixed on these solid phantoms. The type of bolus used was Superflab. 121 TLD chips were placed on the adhesive bolus at 1 cm intervals. Tissue equivalent TLD-100 chips were used to identify measurement points that were easily visible during TPS. Since TLD-100 chips are tissue-equivalent materials, no artefacts occurred. Thus, 121 measurement points were determined on the phantom in a field of  $11 \times 11 \text{ cm}^2$ . The phantom created for point dose measurement is shown in Figure 1. CT images of the created phantom were obtained with a slice thickness of 1 mm. The obtained DICOM images were transferred to TPS.

### Radiotherapy Planning

This study used the Varian DHX (Varian Medical Systems, USA) model linear accelerator device. This device; is a high-tech radiotherapy device that can perform applications such as three-dimensional conformal radiotherapy (3DCRT). In the current Varian DHX device, in the Millennium 80 MLC system, each bank has 40 pairs of leaves and the predicted MLC leaf width in the isocenter is 1 cm. While the SSD distance is 100 cm, the maximum space size opened is  $40 \text{ cm} \times 40 \text{ cm}^2$ . The planning system of this device used in irradiation is Eclipse TPS. This planning system is used to plan the radiotherapy treatments of cancer patients. Eclipse TPS makes dose calculations using a three-dimensional tomography image. Eclipse software is widely used

for planning external treatments using photon, electron and proton beams. In our current research, two different algorithms of Eclipse TPS (Varian Medical Systems, Palo Alto, CA) were used. These were the Pencil Beam Convolution (PBC) and Analytical Anisotropic Algorithm algorithms (AAA). The PBC algorithm is obtained as a result of the integration of all point-spread kernels along the infinite beam path of the photons in the phantom. AAA has been developed for the accuracy of dose distributions and scattered dose calculation in external beam therapy, especially in heterogeneous environments. The current research created beam plans with AAA and PBC algorithms. These plans were for 4x4, 6x6, 8x8, 10x10 and 12x12 cm<sup>2</sup> fields. For each beam field, 100 monitor units (MU) of radiation were applied at 0-degree angle of the Gantry. In addition, irradiation was performed on three different SSDs for different fields determined. The SSD used in the irradiation was 100, 97.5 and 95 cm, respectively. X-ray was applied at 300 MU/min. The beam plans created for different field sizes are shown in Figure 2. The planning made with AAA and PBC algorithms determined 9,25,49,81, and 121 measurement points for 4x4, 6x6, 8x8, 10x10 and 12x12 cm<sup>2</sup> areas, respectively. The point dose was read for each of the determined measuring points.

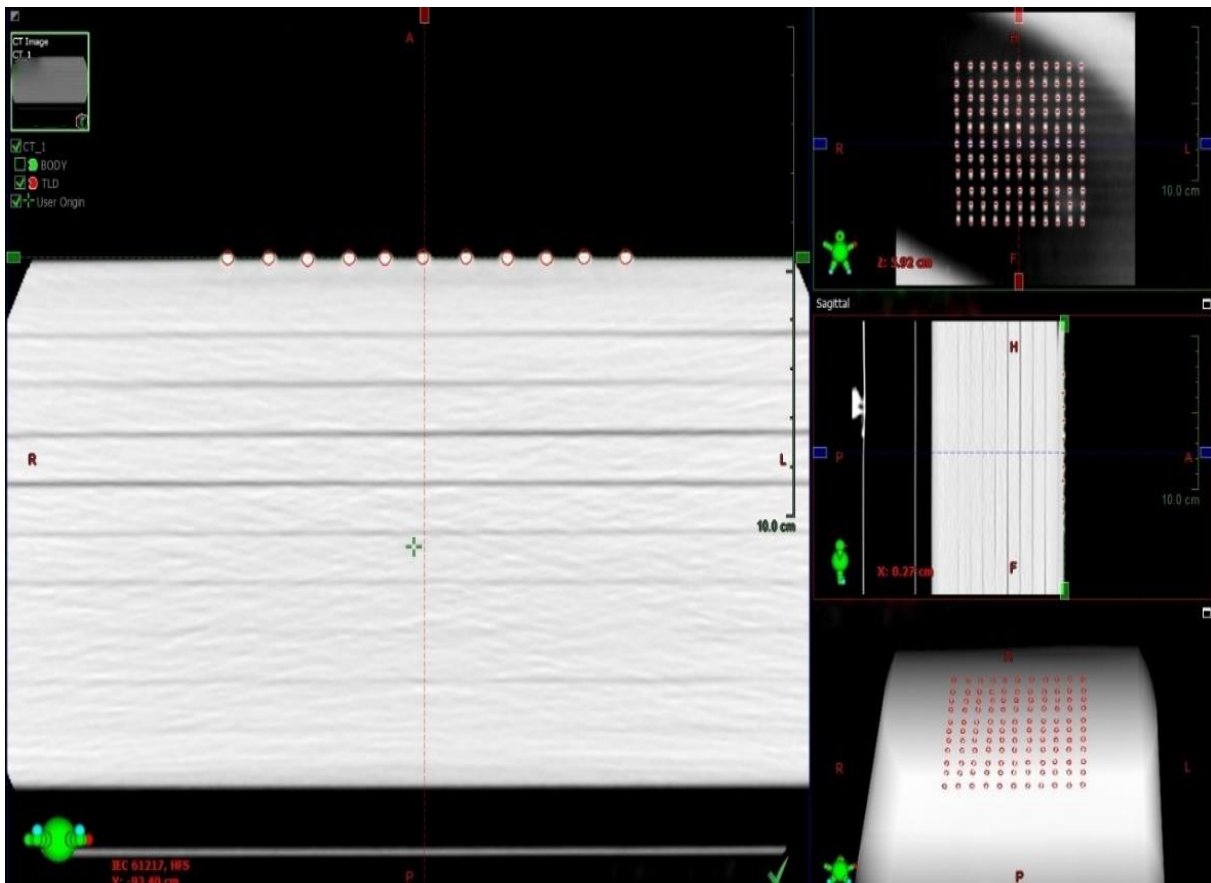


*Figure 1. Phantom created for point dose measurement*

### Calibration of TLDs

Confirmation of the dose calculated by TPS in the surface region was done using thermoluminescence dosimetry (TLD). TLD-100 chips with dimensions of 3.2 mm x 3.2 mm x 0.9 mm were used for surface dose measurement. 190 TLD-100 crystals were used for calibration. First, TLD-100 crystals were numbered and fired in a TLD oven for 1 hour at 400 °C and 2 hours at 100 °C. TLDs were irradiated with 6 MV photon energy in Varian DHX linear accelerator device with one cGy equal to 1MU. Then, preheating was done at 100 °C for 10 minutes in a TLD oven. TLD-100 crystals were read on the Harshaw 3500 TLD reader. Reading calibration factor (RCF) and element correction coefficient (ECC) factors were found for TLDs. Afterwards, 125 TLD-100s with similar dose responses and reproducibility within  $\pm 3\%$  were selected among the ECC values found. TLDs included in the study were irradiated from 80 cGy to 200 cGy, and the calibration curve was drawn. The calibration curve for TLD-100 chips is shown in Figure 3.

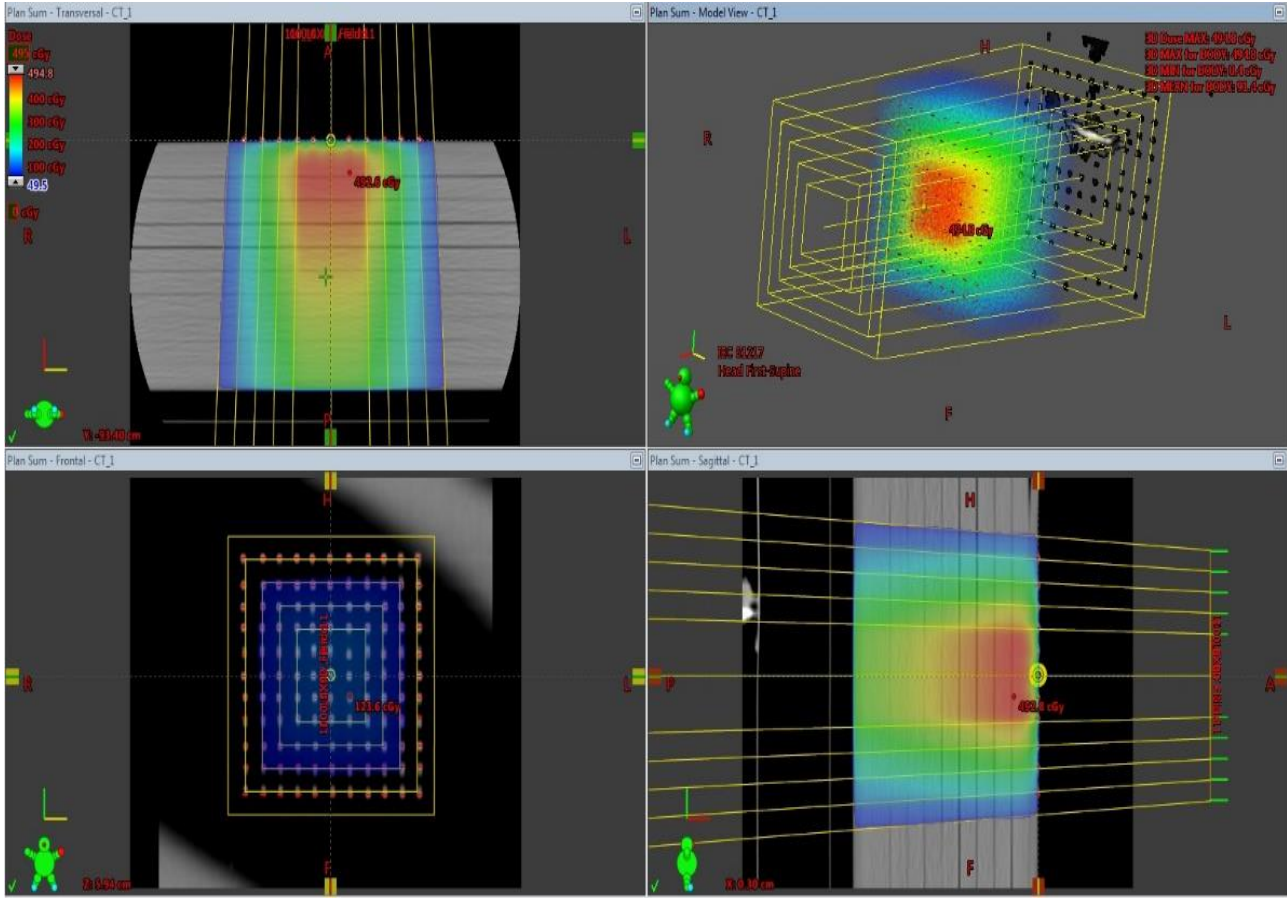


Figure 2. Beam plans created for different field sizes

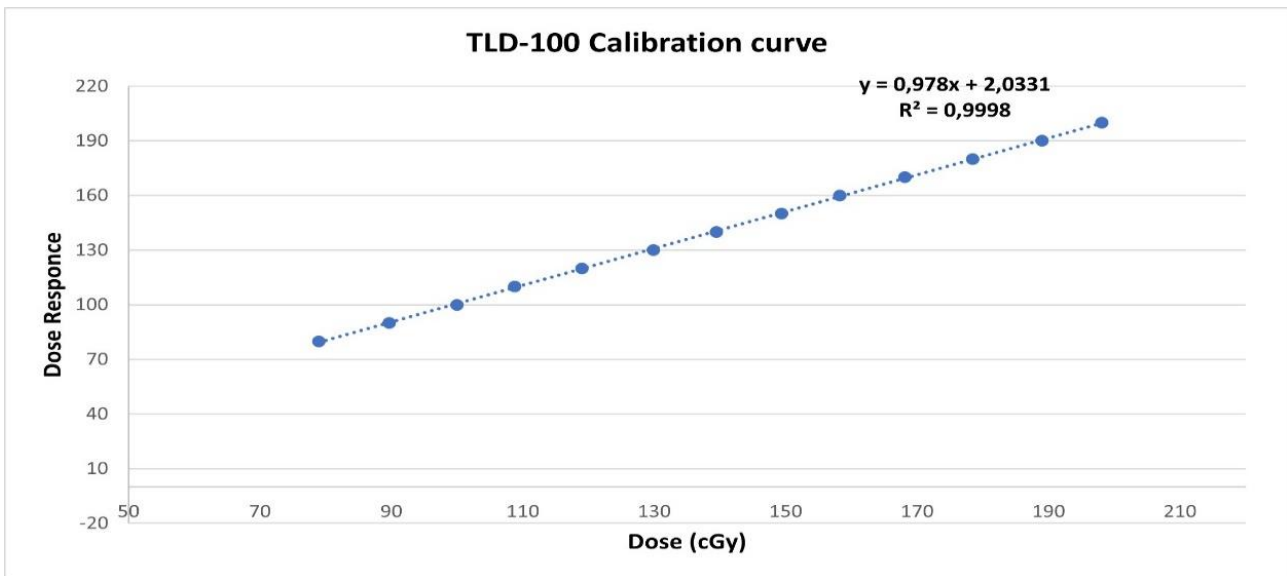


Figure 3. Calibration curve for TLD-100 chips

### Surface Dose Measurement with TLDs

Necessary calibration procedures were performed before proceeding to the measurements in the linear accelerator. Surface doses were measured by TLD according to SSD and field sizes were determined in TPS. The mean dose was measured for each point. For each of the 4x4, 6x6, 8x8, 10x10 and 12x12 cm<sup>2</sup> fields, the TLDs within the field were approximately 1 cm inward from the edge. To measure the effect of SSD on the

surface dose, the isocenter point was placed at 0 cm, 2.5 cm and 5.0 cm depths, respectively. The surface dose at each depth was measured with TLDs. Each measurement was repeated three times to minimize uncertainty.

### Statistical Analysis

Study Statistical Package for Social Sciences, version 25.0 (SPSS, Inc., Chicago, IL) was used for data analysis of the current study. The percentage differences between the point doses calculated by the AAA and PBC algorithms and those measured by TLD were evaluated. Paired Sample t-test for comparison of point doses. used.

### 3. RESULTS AND DISCUSSION

The dose distributions at the measurement points were calculated with AAA and PBC algorithms for different areas and SSDs. Dose distributions at predetermined points were measured with TLDs. Each measurement was repeated three times to minimize uncertainty. The dose distributions calculated by TPS and measured by TLD are shown in Tables 1, 2, and 3 for SSD 100, 97.5 and 95 cm, respectively. Tables 1, 2, and 3 summarise the percentage difference between Eclipse TPS and TLD doses. It was observed that the surface dose increased as the field increased for all SSDs. The AAA algorithm overestimates the surface dose by 4% compared to the TLD measurement for the 4x4 field. The surface dose calculation of the PBC algorithm was found to be high when compared to TLD measurements for all SSDs and fields. There was a significant difference between the PBC algorithm dose calculation and TLD measurements in all fields and SSDs ( $p < 0.001$ ). The highest difference between the PBC algorithm and TLD measurements was 10.23% for SSD=100 and 12x12 field size.

**Table 1.** Surface doses calculated by Eclipse TPS and measured by TLD for SSD 100 cm

Field size (cm <sup>2</sup> )	TLD (cGy)	AAA (cGy)	PBC(cGy)	TLD & AAA		TLD & PBC	
				Diff (%)	p-value	Diff (%)	p-value
4x4	30.24±0.11	31.51±0.23	29.36±0.15	-4.03	<0.001	2.99	<0.001
6x6	33.48±0.08	34.60±0.19	32.25±0.12	-3.24	<0.001	3.81	<0.001
8x8	35.35±0.48	34.97±0.09	33.86±0.08	1.09	<0.001	4.40	<0.001
10x10	38.86±0.20	38.17±1.60	36.66±0.20	1.81	<0.001	6.00	<0.001
12x12	41.59±0.39	39.99±0.17	37.73±0.23	4.00	<0.001	10.23	<0.001

**Table 2.** Surface doses calculated by Eclipse TPS and measured by TLD for SSD 97.5 cm

Field size (cm <sup>2</sup> )	TLD (cGy)	AAA (cGy)	PBC(cGy)	TLD & AAA		TLD & PBC	
				Diff (%)	p-value	Diff (%)	p-value
4x4	31.52±0.09	33.02±0.10	30.44±0.01	-4.54	<0.001	3.54	<0.001
6x6	35.06±0.54	35.39±0.16	32.26±0.21	-0.93	0.007	8.68	<0.001
8x8	38.26±0.38	38.24±0.12	36.36±0.07	0.05	0.798	5.22	<0.001
10x10	42.04±0.22	40.99±0.07	39.73±0.09	2.56	<0.001	5.81	<0.001
12x12	43.49±0.42	42.99±0.06	41.98±0.08	1.63	<0.001	3.60	<0.001

**Table 3.** Surface doses calculated by Eclipse TPS and measured by TLD for SSD 95 cm

Field size (cm <sup>2</sup> )	TLD (cGy)	AAA (cGy)	PBC(cGy)	TLD & AAA		TLD & PBC	
				Diff (%)	p-value	Diff (%)	p-value
4x4	32.41±0.41	34.07±0.06	31.58±0.44	-4.87	<0.001	2.63	0.004
6x6	37.94±0.17	38.02±0.09	35.74±0.27	-0.21	0.073	6.16	<0.001
8x8	42.79±0.05	42.18±0.44	40.91±0.12	1.44	<0.001	4.60	<0.001
10x10	44.68±0.46	43.51±0.30	41.97±0.07	2.69	<0.001	6.46	<0.001
12x12	46.92±0.26	44.90±0.07	43.54±0.21	4.50	<0.001	7.76	<0.001

Mahur et al. (2022) aimed to evaluate the accuracy of the doses calculated by TPS in the surface area of a head and neck phantom they designed, using EBT3 Gafchromic film. In their study, they showed that there was a 16.72% difference between TPS and Gafchromic film measurements for the 3DCRT technique (Mahur et al., 2022). In the current study, all measurements were made with TLDs. Accordingly, the highest difference between Eclipse TPS and TLD measurements was 10.23% for the PBC algorithm. For the AAA algorithm, this difference was 4.87%. In parallel with Mahur et al. (2022), it was observed that TPS could not calculate the surface dose with full accuracy. Oinam and Singh (2010) examined the accuracy of dose calculation in the build-up region of the AAA and PBC algorithms using TLD. They took point dose measurements at different depths near the surface of the head and neck phantom. Oinam and Singh (2010) found a difference of 4.71% and 2.09% for AAA and PBC algorithms, respectively, according to their TLD measurements at a depth of 2 mm from the surface. In this dosimetric study, the surface dose within the build-up region was examined. Accordingly, for all dose measurements, the difference between doses calculated by the AAA algorithm and measured by TLDs was 2.51%. This difference was 5.46% for the PBC algorithm. It was observed that the AAA algorithm was more successful in calculating the surface dose than the PBC algorithm. Wong et al. (2012) evaluated the accuracy of the surface dose estimated by a clinically used TPS on a customised chest wall phantom with TLD measurements. They reported no significant difference between point doses measured by TLD and calculated by TPS, with a difference of up to 2.21% between TPS and TLD doses (Wong et al., 2012). There was no significant difference between TLD measurements and the AAA algorithm in the 8x8 field for SSD 97.5 and the 6x6 field for SSD 95. In parallel with Wong et al. (2012), there was no significant difference in TPS and TLD measurements at different depths and fields. Cao et al. (2017) aimed to evaluate the shallow dose calculation accuracy of four commonly used algorithms with Monte Carlo (MC) simulation and film measurements. When compared with the film measurements, they reported a difference of 4.07% and 22.15% between the AAA and PBC algorithms. They emphasized that caution should be exercised when using AAA and PBC algorithms in superficial dose calculation (Cao et al., 2017). In parallel with Cao et al. (2017), a significant difference was observed between TLD measurements and surface doses calculated by TPS. In particular, it was observed that the PBC algorithm underestimated the surface dose. It was seen that the AAA algorithm can calculate high or low according to the field size. In parallel with Cao et al. (2017), centres using the AAA and PBC algorithms are recommended to be careful about the surface dose.

#### 4. CONCLUSION

This study aimed to give information about the accuracy of surface dose estimation of the commonly used AAA and PBC algorithms in radiotherapy TPS. It was observed that the AAA algorithm performed better in calculating the surface dose than the PBC algorithm. Surface dose calculation performances of AAA and PBC algorithms vary depending on area and SSD. Accurate knowledge of the surface dose can help prevent acute reactions and delayed effects. AAA and PBC algorithm users are advised to be more careful about surface dose calculation.

#### CONFLICT OF INTEREST

The author declares no conflict of interest.

**REFERENCES**

- Aydemir, G. A., Akay, D., Tataroğlu, A., & Ocak, S. B. (2023). Electrical and optical properties of p-Si based structures with lead oxide interfaces. *Materials Science and Engineering: B*, 294, 116552. doi:[10.1016/j.mseb.2023.116552](https://doi.org/10.1016/j.mseb.2023.116552)
- Cao, Y., Yang, X., Yang, Z., Qiu, X., Lv, Z., Lei, M., Liu, G., Zhang, Z., & Hu, Y. (2017). Superficial dose evaluation of four dose calculation algorithms. *Radiation Physics and Chemistry*, 137, 23-28. doi:[10.1016/j.radphyschem.2016.02.032](https://doi.org/10.1016/j.radphyschem.2016.02.032)
- Chakarova, R., Gustafsson, M., Back, A., Drugge, N., Palm, Å., Lindberg, A., & Berglund, M. (2012). Superficial dose distribution in breast for tangential radiation treatment, Monte Carlo evaluation of Eclipse algorithms in case of phantom and patient geometries. *Radiotherapy and Oncology*, 102(1), 102-107. doi:[10.1016/j.radonc.2011.06.021](https://doi.org/10.1016/j.radonc.2011.06.021)
- Córdoba, E. E., Lacunza, E., & Güerci, A. M. (2021). Clinical factors affecting the determination of radiotherapy-induced skin toxicity in breast cancer. *Radiation Oncology Journal*, 39(4), 315-323. doi:[10.3857/roj.2020.00395](https://doi.org/10.3857/roj.2020.00395)
- Danckaert, W., Ost, P., & De Wagter, C. (2023). Accuracy and reliability of a commercial treatment planning system in nontarget regions in modern prostate radiotherapy. *Journal of Applied Clinical Medical Physics*, 24(8). doi:[10.1002/acm2.14003](https://doi.org/10.1002/acm2.14003)
- Guardiola, C., Bachiller-Perea, D., Kole, E. M. M., Fleta, C., Quirion, D., De Marzi, L., & Gómez, F. (2022). First experimental measurements of 2D microdosimetry maps in proton therapy. *Medical Physics*, 50(1), 570-581. doi:[10.1002/mp.15945](https://doi.org/10.1002/mp.15945)
- Lejosne, S., Allison, H. J., Blum, L. W., Drozdov, A. Y., Hartinger, M. D., Hudson, M. K., Jaynes, A. N., Ozeke, L., Roussos, E., & Zhao, H. (2022). Differentiating Between the Leading Processes for Electron Radiation Belt Acceleration. *Frontiers in Astronomy and Space Sciences*, 9. doi:[10.3389/fspas.2022.896245](https://doi.org/10.3389/fspas.2022.896245)
- Mahur, M., Singh, M., Semwal, M., & Gurjar, O. (2022). Evaluation of surface dose calculations using monaco treatment planning system in an indigenously developed head and neck phantom. *Medical Journal of Dr. D.Y. Patil Vidyapeeth*. doi:[10.4103/mjdrdypu.mjdrdypu\\_827\\_21](https://doi.org/10.4103/mjdrdypu.mjdrdypu_827_21)
- Matsumoto, T., Toya, R., Shimohigashi, Y., Watakabe, T., Matsuyama, T., Saito, T., Fukugawa, Y., Kai, Y., & Oya, N. (2021). Plan Quality Comparisons Between 3D-CRT, IMRT, and VMAT Based on 4D-CT for Gastric MALT Lymphoma. *Anticancer Research*, 41(8), 3941-3947. doi:[10.21873/anticancer.15190](https://doi.org/10.21873/anticancer.15190)
- Mowery, M. L., & Singh, V. (2023). *X-ray Production Technical Evaluation*. StatPearls. Treasure Island (FL).
- Ng, K.-H., Ung, N. M., & Hill, R. (2022). *Problems and Solutions in Medical Physics: Radiotherapy Physics*. CRC Press.
- Oinam, A. S., & Singh, L. (2010). Verification of IMRT dose calculations using AAA and PBC algorithms in dose buildup regions. *Journal of Applied Clinical Medical Physics*, 11(4), 105-121. doi:[10.1120/jacmp.v11i4.3351](https://doi.org/10.1120/jacmp.v11i4.3351)
- Panettieri, V., Barsoum, P., Westermarck, M., Brualla, L., & Lax, I. (2009). AAA and PBC calculation accuracy in the surface build-up region in tangential beam treatments. Phantom and breast case study with the Monte Carlo code PENelope. *Radiotherapy and Oncology*, 93(1), 94-101. doi:[10.1016/j.radonc.2009.05.010](https://doi.org/10.1016/j.radonc.2009.05.010)
- Ramseier, J. Y., Ferreira, M. N., & Leventhal, J. S. (2020). Dermatologic toxicities associated with radiation therapy in women with breast cancer. *International Journal of Women's Dermatology*, 6(5), 349-356. doi:[10.1016/j.ijwd.2020.07.015](https://doi.org/10.1016/j.ijwd.2020.07.015)
- Ravikumar, M., & Ravichandran, R. (2000). Dose measurements in the build-up region for the photon beams from Clinac-1800 dual energy medical linear accelerator. *Strahlentherapie und Onkologie*, 176(5), 223-228. doi:[10.1007/s000660050004](https://doi.org/10.1007/s000660050004)
- Simoni, N., Micera, R., Paiella, S., Guariglia, S., Zivelonghi, E., Malleo, G., Rossi, G., Addari, L., Giuliani, T., Pollini, T., Cavedon, C., Salvia, R., Milella, M., Bassi, C., & Mazzarotto, R. (2021). Hypofractionated Stereotactic Body Radiation Therapy With Simultaneous Integrated Boost and Simultaneous Integrated

Protection in Pancreatic Ductal Adenocarcinoma. *Clinical Oncology*, 33(1), e31-e38. doi:[10.1016/j.clon.2020.06.019](https://doi.org/10.1016/j.clon.2020.06.019)

Tsapaki, V., & Bayford, R. (2015). Medical Physics: Forming and testing solutions to clinical problems. *Physica Medica*, 31(7), 738-740. doi:[10.1016/j.ejmp.2015.05.017](https://doi.org/10.1016/j.ejmp.2015.05.017)

Wang, K., & Tepper, J. E. (2021). Radiation therapy-associated toxicity: Etiology, management, and prevention. *CA: A Cancer Journal for Clinicians*, 71(5), 437-454. doi:[10.3322/caac.21689](https://doi.org/10.3322/caac.21689)

Wong, S., Back, M., Tan, P. W., Lee, K. M., Baggarley, S., & Lu, J. J. (2012). Can radiation therapy treatment planning system accurately predict surface doses in postmastectomy radiation therapy patients? *Medical Dosimetry*, 37(2), 163-169. doi:[10.1016/j.meddos.2011.06.006](https://doi.org/10.1016/j.meddos.2011.06.006)